# A first-principles study of B2 NiAl alloyed with rare earth elements Pr, Pm, Sm, and Eu*

He Jun-Qi(何君琦)†, Wang You(王 铀)‡, Yan Mu-Fu(闫牧夫), Pan Zhao-Yi(潘兆义), and Guo Li-Xin(郭立新)

*School of Materials Science and Engineering, Harbin Institute of Technology, Harbin* 150001, *China*

(Received 11 June 2012; revised manuscript received 26 July 2012)

The structural, elastic, and electronic properties of NiAl alloyed with rare earth elements Pr, Pm, Sm, and Eu are investigated by using density functional theory (DFT). The study suggests that Pr, Pm, Sm, and Eu all tend to be substituted for an Al site. $Ni_8Al_7Pm$ possesses the largest ductility. Only the hardness and ductility of $Ni_8Al_7Eu$ are enhanced simultaneously. The covalency strength of the Ni–Al bond in $Ni_8Al_7Pm$ is higher than that in $Ni_8Al_7Eu$. The covalency strength of an Al–Al bond and that of a Ni–Ni bond in $Ni_8Al_7Eu$ are higher than that in $Ni_8Al_7Pm$. The Ni–Pm bond and the Ni–Eu bond are covalent, and the covalency strength of the Ni–Pm bond is greater. The Al–Pm bond and the Al–Eu bond show great covalency strength and ionicity, respectively.

**Keywords:** first-principles, intermetallics, rare earth element, electronic structure

**PACS:** 71.15.Mb, 71.20.Lp, 71.20.–b **DOI:** 10.1088/1674-1056/22/2/027102

## 1. Introduction

Nickel–aluminum alloys are remarkable for their attractive properties including good high-temperature strength, resistance to oxidation and corrosion, relatively low material density and high melting point, thus constituting an important area of material science research in both experimental and modeling communities.[1,2] However, the application of NiAl is restricted due to its brittle fracture and low tensile ductility at room temperature.[3]

Alloying as an effective method is widely studied,[4,5] even to improve the quality of NiAl.[6,7] Alloying elements Ti, Zr, Hf, Nb, and Ta each have a low solubility in NiAl and exist in the form of ternary intermetallic compounds such as Heusler phase and Laves phase. V, Cr, Mo, and W can form pseudobinary eutectic systems with NiAl. Iron, Co, and Cu each have high solubility in NiAl. The most common ternary elements are 3d and 4d transitional elements like Fe, Cr, Co, Mo, Ti, Ga, and Mn, and they have been studied extensively using both experimental and theoretical methods.[8–10]

Rare earth elements (REEs) are surface-active. An appropriate amount of an REE additive (like Nd Y, Ce, Nd, and Dy) can improve the room temperature compressive ductility of an alloy,[11,12] even the *RM* (where *R* denotes a rare-earth element and *M* refers to a late transition metal or an early p-element) intermetallics exhibit distinctly different ductility behavior.[13]

However, the research of NiAl alloyed with Pr, Pm, Sm, and Eu is still limited. Moreover, the studies of Pr, Pm, Sm, and Eu addition at an atomic level are not sufficient, and the effect of these REEs on the ductility, especially the micromechanism of the interaction between NiAl and the adding REEs is not clear. In this study, a first-principles approach is used to investigate the structural, elastic, and electronic properties of NiAl alloyed with Pr, Pm, Sm, and Eu in order to illuminate the intrinsic effect of REEs.

## 2. Computational method

In the calculation of density functional theory (DFT) we employ the plane-wave total-energy method in the generalized gradient approximation (GGA) described by Perdew *et al*.[14] for exchange correlation as implemented in the Cambridge Sequential Total Energy Package (CASTEP) code.

This program is employed to investigate the lattice parameters, elastic characteristics, and electronic structures of the NiAl $2\times2\times2$ supercell with addition of REEs. The unit cell of NiAl with space group *PM*-3*M* and lattice constant 2.9 Å (1 Å = 0.1 nm) is established, which is composed of one Ni atom at (1/2, 1/2, 1/2) and one Al atom at (0, 0, 0). The values of kinetic energy cutoff $E_{\rm cut}$ and the number of *K*-points are tested as 310 eV, 330 eV, 350 eV, 370 eV, 390 eV and $1\times1\times1$, $2\times2\times2$, $3\times3\times3$, $4\times4\times4$, $5\times5\times5$ until the calculated energy converges within the required tolerance, where $E_{\rm cut}$ determines the number of plane waves, and the sampling of the irreducible wedge of the Brillouin zone is implemented at *K* points. $E_{\rm cut}$ is set to be 350 eV and the number of *k* points is set to be $4\times4\times4$ with a regular Monkhorst–Pack scheme

*Project supported by the National Natural Science Foundation of China (Grant No. 50871035) and the Program of Excellent Team at Harbin Institute of Technology, China.

†Corresponding author. E-mail: hejunqi1108@163.com

‡Corresponding author. E-mail: wangyou@hit.edu.cn

© 2013 Chinese Physical Society and IOP Publishing Ltd 

according to the testing results. In the calculation of self-consistent field (SCF), the Pulay scheme of density mixing[15] is adopted. The calculations of the elastic constant and the electronic structure are followed by cell optimization with a convergence tolerance of energy of $5.0\times10^{-6}$ eV·atom$^{-1}$, a maximum displacement of $5.0\times10^{-4}$ Å and a maximum force of 0.01 eV·Å$^{-1}$. A supercell model of NiAl with REE Eu/Pm, which consists of 16 atoms, is shown in Fig. 1.

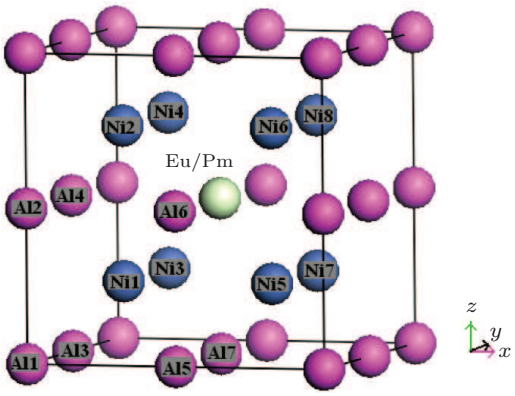



**Fig. 1.** (color online) Model of $Ni_8Al_7Eu$/$Ni_8Al_7Pm$. The rare earth element Eu/Pm is placed in the centre of the supercell, substituted for Al.

## 3. Results and discussion

### 3.1. Site preferences of Pr, Pm, Sm, and Eu in NiAl

Formation enthalpy is used to choose the more stable site that REE $M$ occupies (Ni site or Al site) in NiAl. The site preference energy is described as

$$E_{\text{site}} = E_1 - E_2, \tag{1}$$

where $E_1$ and $E_2$ are formation enthalpies of $Ni_7Al_8M$ and $Ni_8Al_7M$, respectively. The usual definition of formation enthalpy is the total energy difference between compound and constituent elements in the solid state, so $E_1$ and $E_2$ are expressed as[16]

$$E_1 = E_{Ni_7Al_8M} - 7E_{\text{Ni}} - 8E_{\text{Al}} - E_M, \tag{2}$$

$$E_2 = E_{Ni_8Al_7M} - 8E_{\text{Ni}} - 7E_{\text{Al}} - E_M. \tag{3}$$

Here, $E_{\text{Ni}}$, $E_{\text{Al}}$, and $E_M$ are the total energies of pure Ni, Al, and $M$, respectively. So we can deduce the form of $E_{\text{site}}$ from the above two formation energies as follows:

$$E_{\text{site}} = E_1 - E_2 = E_{Ni_7Al_8M} - E_{Ni_8Al_7M} + E_{\text{Ni}} - E_{\text{Al}}. \tag{4}$$

If $E_{\text{site}} < 0$, substitution for Ni is more favorable, and if $E_{\text{site}} > 0$, $M$ is on the Al site. The formation energies of face-centred cubic (fcc) Al and Ni are calculated, and their values are $-56.999$ eV and $-1356.188$ eV, respectively.

The total energies of $E_{Ni_7Al_8M}$ and $E_{Ni_8Al_7M}$, and site preference energy are shown in Table 1. It can be seen from the values of $E_{\text{site}}$ that Pr, Pm, Sm, and Eu are all tend to be substituted for Al site. Their site preference energies increase gradually, and the models $Ni_8Al_7Pr$, $Ni_7Al_8Pm$, $Ni_8Al_7Sm$, and $Ni_7Al_8Eu$ are used for the following calculation.

**Table 1.** Total energies of $E_{Ni_7Al_8M}$ and $E_{Ni_8Al_7M}$ (in eV), which represents the values of site preference energy $E_{\text{site}}$ (in eV), and site preferences.

| $M$ | $E_{Ni_7Al_8M}$ | $E_{Ni_8Al_7M}$ | $E_{\text{site}}$ | Site preference |
|---|---|---|---|---|
| Pr | –11234.0761 | –12533.6252 | 0.3605 | Al |
| Pm | –11805.6852 | –13105.2787 | 0.4049 | Al |
| Sm | –12143.3072 | –13442.9709 | 0.4751 | Al |
| Eu | –12521.0742 | –13820.9165 | 0.6537 | Al |

### 3.2. Lattice parameter

The lattice parameters of models doped with different REEs are shown in Table 2. The equilibrium lattice constant is set to be 5.8 Å, which comes from the experimental results.[17,18] In Table 2, the lattice parameters increase to different extents after alloying with REEs. Among these models, $Ni_8Al_7Sm$ exhibits the largest change in equilibrium lattice constant, and the rest of the alloying models present almost the same changes.

**Table 2.** Equilibrium lattice constants in $Ni_7Al_8M$ and $Ni_8Al_7M$ and their changes. $\delta = (a-5.8)/5.8$.

| Model | $a$/Å | $\delta$/% |
|---|---|---|
| $Ni_8Al_8$ | 5.80 | 0 |
| $Ni_8Al_7Pr$ | 5.98 | 3.10 |
| $Ni_8Al_7Pm$ | 5.98 | 3.10 |
| $Ni_8Al_7Sm$ | 5.99 | 3.28 |
| $Ni_8Al_7Eu$ | 5.98 | 3.10 |

### 3.3. Elastic properties

The elastic properties of single crystals are described by the elements $C_{ij}$ of elasticity tensor. The independent elastic constants in the cubic phase are $C_{11}$, $C_{12}$, and $C_{44}$, from which we can obtain bulk modulus $B_0$, shear modulus $G$, Young's modulus $E$, and the Poisson ratio $\nu$: [19]

$$B_0 = (C_{11} + 2C_{12})/3, \tag{5}$$

$$G = (3C_{44} + C_{11} - C_{12})/5, \tag{6}$$

$$E = 9B_0G/(3B_0 + G), \quad \nu = (1 - E/3B_0)/2. \tag{7}$$

The elastic constants $C_{11}$, $C_{12}$, $C_{44}$, and $C_{11}$–$C_{12}$ are shown in Table 3. From the data of $Ni_8Al_8$, we can see that our results are in good agreement with the experimental ones.[20,21] The mechanical stability criteria in cubic crystal are $C_{11}$–$C_{12} > 0$, $C_{44} > 0$, and $B_0 > 0$.[22,23] The calculated elastic constants show that the models of $Ni_8Al_7Pr$, $Ni_8Al_7Pm$, $Ni_8Al_7Sm$, and $Ni_8Al_7Eu$ are all stable.

**Table 3.** Values of the elastic constants $C_{11}$, $C_{12}$, $C_{44}$, and $C_{11}$–$C_{12}$ of all supercells.

| Model | $C_{11}$/GPa | $C_{12}$/GPa | $C_{44}$/GPa | $C_{11}$–$C_{12}$ |
|---|---|---|---|---|
| $Ni_8Al_8$ (Exp) | 199 | 137 | 116 | 62 |
| $Ni_8Al_8$ (Exp) | 204.6 | 135.4 | 116.8 | 69.2 |
| $Ni_8Al_8$ | 173.48 | 149.37 | 117.41 | 24.21 |
| $Ni_8Al_7Pr$ | 199.41 | 108.92 | 38.34 | 90.49 |
| $Ni_8Al_7Pm$ | 310.59 | 207.62 | 79.00 | 102.97 |
| $Ni_8Al_7Sm$ | 329.57 | 170.89 | 69.56 | 158.68 |
| $Ni_8Al_7Eu$ | 331.73 | 173.65 | 114.11 | 158.08 |

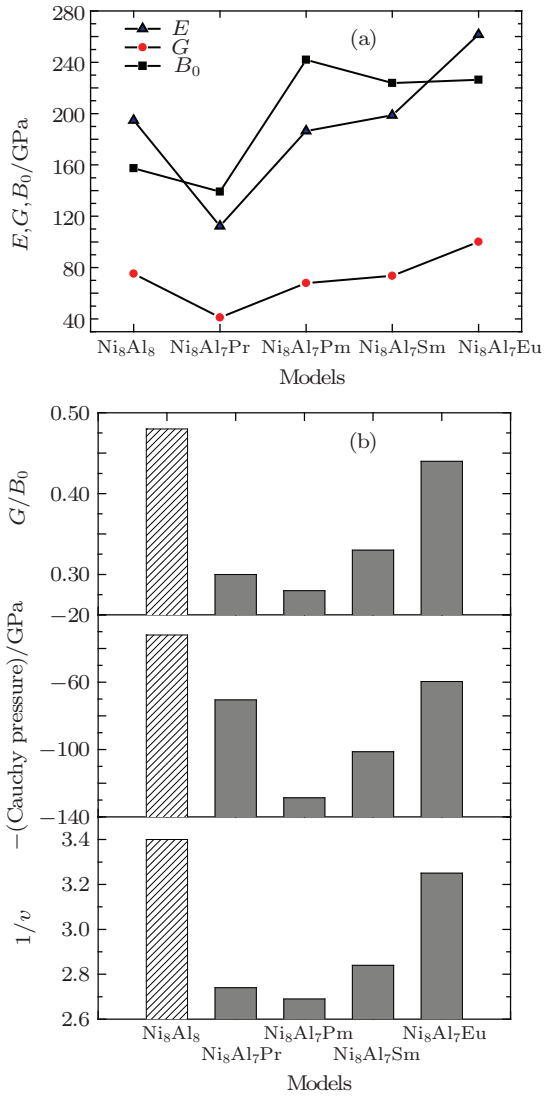



**Fig. 2.** (color online) (a) The curves of Young's modulus $E$, shear modulus $G$, and bulk modulus $B_0$, and (b) the ratios of shear modulus to bulk modulus $G/B_0$, negative Cauchy pressure parameters $-(C_{12}-C_{44})$, and the reciprocal of Poisson's ratio $1/v$ of several different models.

In Fig. 2 the Young's modulus $E$, shear modulus $G$, bulk modulus $B_0$, negative Cauchy pressure $-(C_{12}-C_{44})$, $G/B_0$, and $1/v$ are calculated and shown in the order of alloying elements Pr, Pm, Sm, and Eu. Figure 2(a) shows the curves of $E$, $G$, and $B_0$ of their models. It is generally believed that the hardness of material is related to its elastic modulus, such as the Young's modulus $E$, and the shear modulus $G$.[24] Although the relationships between hardness and the modulus are not identical for different materials, the general trend is that the larger the modulus, the harder the material is. Therefore, the calculated Young's modulus can be used as a general guidance for the selection of materials. The bulk modulus $B_0$ represents the resistance to volume change and is related to overall atomic binding properties in a material. From Fig. 2(a) it can be seen that $E$ and $G$ follow the similar trends. The $E$ values of $Ni_8Al_7Sm$ and $Ni_8Al_7Eu$ are larger than that of $Ni_8Al_8$, and that the $Ni_8Al_7Eu$ possesses the largest $E$ value. The $G$ value of the $Ni_8Al_7Eu$ is greater than that of the $Ni_8Al_8$. The $B_0$ values of the $Ni_8Al_7Pm$, $Ni_8Al_7Sm$, and $Ni_8Al_7Eu$ are enhanced compared with that of $Ni_8Al_8$. So, alloying with Eu enhances the Young's modulus $E$ and the shear modulus $G$ of NiAl simultaneously, thus the hardness of the $Ni_8Al_7Eu$ is greater than that of the $Ni_8Al_8$. Moreover, the $Ni_8Al_7Eu$ exhibits the largest atomic binding properties.

Figure 2(b) shows the results of the reciprocal of Poisson's ratio $1/v$, negative Cauchy pressure $-(C_{12}-C_{44})$, and the ratio of shear modulus to bulk modulus $G/B_0$. Poisson's ratio reflects the stability of a crystal against shear. This ratio can formally take values between $-1$ and 0.5, the smaller the Poisson's ratio, the more brittle behavior of materials will be obtained. In other words, the smaller the reciprocal of Poisson's ratio $1/v$, the more ductile the material is. Cauchy pressure as an evaluation norm for ductile or brittle material, generally, for ductile material is positive, and it is negative for brittle material. Figure 2(b) shows negative Cauchy pressure for easy comparison, the smaller negative Cauchy pressure represents relative ductile material. Pugh[25] has proposed a simple relationship that empirically the plastic property of metal is related to its elastic modulus by $G/B_0$. If $G/B_0 < 0.5$, the material behaves as a ductile matter, otherwise, a brittle matter. From Fig. 2(b), we can conclude that all the alloying REEs have improved the ductility of NiAl, and the $Ni_8Al_7Pm$ possesses the largest ductility while its hardness is a little lower than that of $Ni_8Al_8$. Only the hardness and ductility of $Ni_8Al_7Eu$ are enhanced simultaneously compared with those of $Ni_8Al_8$, while its ductility is lower than that of $Ni_8Al_7Pm$.

### 3.4. Density of states (DOS) and populations

Pm and Eu are two representative alloying elements among the four REEs as discussed above, we compare the density of states (DOS) of $Ni_8Al_8$ with those of the $Ni_8Al_7Pm$ and $Ni_8Al_7Eu$ in order to find the effects of REEs Pm and Eu on the electronic properties of NiAl.

The dominant feature of the $Ni_8Al_8$ DOS is the existence of sharp peaks contributed by d orbitals of Ni, which hybridize weakly with the p orbitals of Al as shown in Fig. 3(a). The DOS of $Ni_8Al_7Pm$, shown in Fig. 3(b), has two additional sharp peaks around $-18$ eV and $-38$ eV, which are mainly due to the contributions of s and p orbitals of Pm. Because these orbitals are the inner electron orbitals, they have weak inter-

actions with electrons of other atoms. The DOS of $Ni_8Al_7Eu$ shown in Fig. 3(c) shifts the two sharp peaks toward lower energy. Near the Fermi level, the conduction bands of $Ni_8Al_7Pm$ and $Ni_8Al_7Eu$ narrow, which is due to the fact that the difference between the number of p electrons of Al and that of f electrons of Pm (or Eu) leads to their different contributions to the DOS, meanwhile, the hybridization between f electrons of Pm (or Eu) and outer electrons of Al plays a big role.

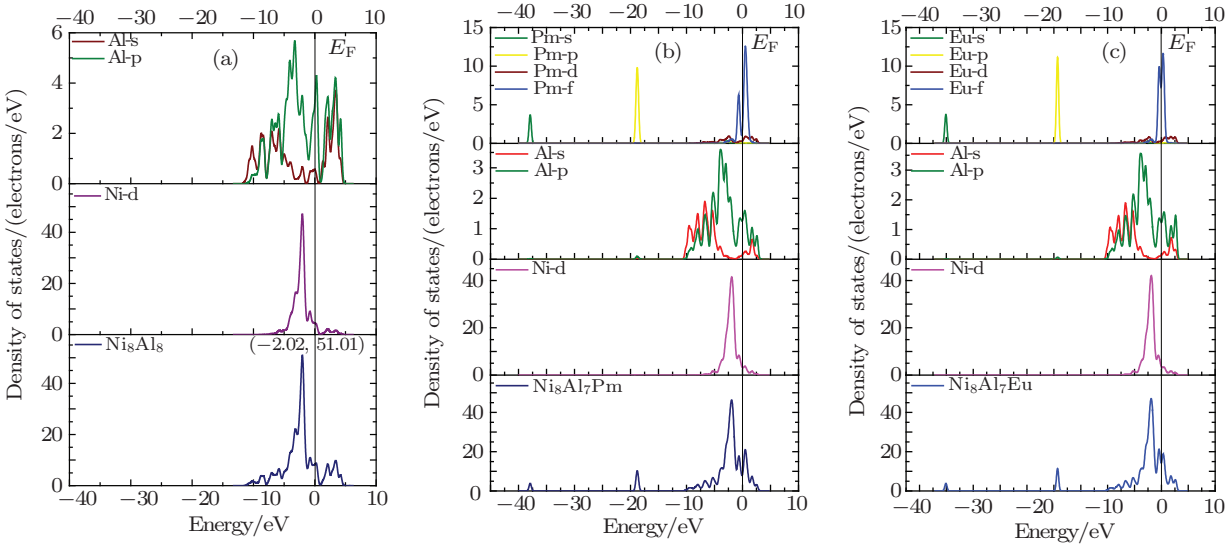



**Fig. 3.** (color online) Densities of states (DOSs) of (a) $Ni_8Al_8$, (b) $Ni_8Al_7Pm$, and (c) $Ni_8Al_7Eu$.

The bond populations indicate the overlap degree of the electron clouds of two bonding atoms and can be used to access covalent or ionic nature of a chemical bond. For the bond populations, the lowest and highest values imply that the chemical bond exhibits strong ionicity and covalency, respectively.

$Ni_8Al_8$ model is presented for comparison. In $Ni_8Al_8$, three Ni atoms located, respectively, at the corner, on the edge and in the face can represent corresponding situations of Ni atoms. The population values of the Ni–Al bonds are the same, Al–Al bonds (or Ni–Ni bonds) are formed by each single Al atom (or Ni atom) and its three nearest neighbor Ni atoms (or Al atoms). All the populations of Al–Al bonds or Ni–Ni bonds are the same.

In $Ni_8Al_7Pm$ and $Ni_8Al_7Eu$, for Ni–Al bonds, because of the symmetry of the supercell, $Ni_1$ and $Al_1$, $Al_2$, $Al_4$ located, respectively, at the corner, on the edge and in the face can represent corresponding situations of Ni–Al bonds. As for Al–Al bonds, there are two situations "corner–edge" and "edge–face", so $Al_1$–$Al_2$ and $Al_2$–$Al_4$ represent the Al–Al bonds in $Ni_8Al_7Pm$ and $Ni_8Al_7Eu$, respectively. Ni–Ni bonds are all along the axis direction just like that in $Ni_8Al_8$, and the populations are the same. Ni/Al-REE bonds are REE with their nearest Ni/Al atoms.

From Table 4, for Ni–Al bonds, the values of $P$ in $Ni_8Al_7Pm$ are increased to various extents compared with those in $Ni_8Al_8$, while in $Ni_8Al_7Eu$, the values for, such as, $Ni_1$–$Al_1$ bonds are partially reduced. While the average value of $Ni_8Al_7Pm$ is less than that of $Ni_8Al_7Eu$, so the covalency strength of Ni–Al bond in $Ni_8Al_7Eu$ is greater than that in $Ni_8Al_7Pm$. For Al–Al bonds, after alloying with an REE, the values of $P$ in these two supercells show the trend of partial increase and that of partial decrease, and the covalency strength of Ni–Al bond in $Ni_8Al_7Pm$ is larger than that in $Ni_8Al_7Eu$, hence the covalency strength of Al–Al bond in $Ni_8Al_7Pm$ is larger than that in $Ni_8Al_7Eu$. For Ni–Ni bond, the value of $P$ in $Ni_8Al_8$ is negative, while alloying with an REE, the values in both the two supercells are positive, and the covalency strength

**Table 4.** Charge populations of unit bond length in $Ni_8Al_7Pm$, $Ni_8Al_7Eu$, and $Ni_8Al_8$.

| Bond ($Ni_8Al_7Pm$) | Population | Length/Å | $P$ (charge/nm) |
|---|---|---|---|
| Ni1–Al1 | 0.14 | 2.44829 | 0.57183 |
| Ni1–Al2 | 0.27 | 2.54955 | 1.05901 |
| Ni1–Al4 | 0.29 | 2.66067 | 1.08995 |
| Al1-Al2 | 0.18 | 2.99683 | 0.60063 |
| Al2-Al4 | 0.27 | 2.98936 | 0.90320 |
| Ni–Ni | 0.19 | 2.82686 | 0.67212 |
| Ni–Pm | 1.31 | 2.73392 | 4.79165 |
| Al–Pm | 0.99 | 2.99183 | 3.30901 |
| Bond ($Ni_8Al_7Eu$) | Population | Length/Å | $P$ (charge/nm) |
| Ni1–Al1 | 0.13 | 2.44821 | 0.531000 |
| Ni1–Al2 | 0.27 | 2.53703 | 1.064237 |
| Ni1–Al4 | 0.30 | 2.64028 | 1.136243 |
| Al1–Al2 | 0.17 | 2.99105 | 0.568362 |
| Al2–Al4 | 0.25 | 2.99182 | 0.835827 |
| Ni–Ni | 0.18 | 2.82372 | 0.637457 |
| Ni–Eu | 0.18 | 2.73346 | 0.658506 |
| Al–Eu | –0.97 | 2.99121 | –3.242835 |
| Bond ($Ni_8Al_8$) | Population | Length/Å | $P$ (charge/nm) |
| Ni–Al | 0.14 | 2.51147 | 0. 557442 |
| Al–Al | 0.22 | 2.90000 | 0.758621 |
| Ni–Ni | –0.03 | 2.90000 | –0.103448 |

of the Ni–Ni bond in $Ni_8Al_7Pm$ is larger than that in $Ni_8Al_7Eu$. For Ni-REE bonds, all the values of $P$ in $Ni_8Al_7Pm$ and $Ni_8Al_7Eu$ are positive, however, the value of Ni–Pm bond length is larger than that of the Ni–Eu bond; Ni–Pm possesses a higher covalency strength. About Al–REE bonds, the values of $P$ are positive in $Ni_8Al_7Pm$ and negative in $Ni_8Al_7Eu$, hence, Al–Pm bonds show a great covalency strength and Al–Eu bonds exhibit strong ionicity.

Therefore, it can be concluded that the covalency strengths of Ni–Al bonds in $Ni_8Al_7Pm$ are totally increased while in $Ni_8Al_7Eu$ are partially reduced; for the covalency strengths of Al–Al bonds, in both $Ni_8Al_7Pm$ and $Ni_8Al_7Eu$, some are partially reduced and some partially increased, the magnitude of change in $Ni_8Al_7Pm$ is greater; Ni–Ni bonds in the two supercells both present covalency, whose strength in $Ni_8Al_7Pm$ is slightly larger; Ni–Pm bonds and Ni–Eu bonds present covalency, and the covalency strength of Ni–Pm bond is greater; Al–Pm and Al–Eu show great covalency strength and iconicity values, respectively.

## 4. Conclusions

*Ab initio* density functional theory calculations are performed to study the effects of rare earth alloying elements (Pr, Pm, Sm, and Eu) on the crystal structural, elastic, and electronic properties of NiAl. In general, the following conclusions are obtained. (i) Pr, Pm, Sm, and Eu all tend to be substituted for an Al site. (ii) $Ni_8Al_7Pm$ possesses the largest ductility while its hardness is a little lower than that of $Ni_8Al_8$. Only the hardness and ductility of $Ni_8Al_7Eu$ are enhanced simultaneously compared with those of $Ni_8Al_8$, while its ductility is lower than that of $Ni_8Al_7Pm$. (iii) The covalency strength of Ni–Al bond in $Ni_8Al_7Pm$ is larger than that in $Ni_8Al_7Eu$. On the contrary, the covalency strengths of Al–Al and Ni–Ni bond in $Ni_8Al_7Eu$ are larger than those in $Ni_8Al_7Pm$; Ni–Pm bonds and Ni–Eu bonds present covalency, and the covalency strength of Ni–Pm bond is greater; Al–Pm and Al–Eu show great covalency strengths and iconicity values, respectively.

## References


[1] Guo J T, Huai K W, Gao Q, Ren W L and Li G S 2007 *Intermetallics* **15** 727
[2] Xu Q C and Ven A V 2011 *Acta Materialia* **59** 95
[3] Liu C T, Stringer J and Mundy J N 1997 *Intermetallics* **5** 579
[4] Xu G G, Wu J, Chen Z G, Lin Y B and Huang Z G 2012 *Chin. Phys.* B **21** 097401
[5] Haq B U, Afaq A, Ahmed R and Naseem S 2012 *Chin. Phys.* B **21** 097101
[6] Albiter A, Salazar M, Bedolla E and Drew R J 1997 *Mater. Sci. Eng*. A **347** 154
[7] Chung C Y, Xie C Y and Hsu T Y 1997 *Scripta. Mater.* **37** 99
[8] Kovalev A I, Barskaya R A and Wainstein D L 2003 *Surf. Sci.* **532–535** 35
[9] Lazar P and Podloucky R 2006 *Phys. Rev*. B **73** 1
[10] Fu C L, Liu C T and Wang X L 2004 *Intermetallics* **12** 911
[11] Ren W L, Guo J T, Li G S and Zhou J Y 2003 *Mater. Lett.* **57** 1374
[12] Chen W, Hines J R and Wang Y 2004 *Adv. Eng. Mater.* **6** 876
[13] Wu X Z, Wang S F and Liu R P 2009 *Chin. Phys.* B **18** 2905
[14] Monkhorst H J and Pack J D 1976 *Phys. Rev.* B **13** 5188
[15] Hammer B, Hansen L B and Nørskov J K 1999 *Phys. Rev.* B **59** 7413
[16] Wolf W, Podloucky R and Rogl P 1996 *Intermetallics* **4** 201
[17] Perdew J P, Burke K and Ernzerhof M 1996 *Phys. Rev. Lett.* **77** 3865
[18] Chen K Y, Zhao L and John R J 2003 *Physica* D: *Appl. Phys.* **36** 2725
[19] Chen K Y and Zhao L R 2003 *J. Appl. Phys.* **93** 2414
[20] Davenport T, Zhou L and Trivisonno J 1999 *Phys Rev.* B **59** 3421
[21] Farkas D, Mutasa B and Vailhe C 1995 *Model. Simul. Mater. Sci. Eng.* **3** 201
[22] Nye J F 1985 *Physical Properties of Crystals* (Oxford: Oxford University Press)
[23] Karki B B, Ackland G J and Crain J 1997 *J. Phys: Condens. Matter.* **9** 8579
[24] Frantsevich I N, Voronov F F and Bokuta S A 1983 *Elastic Constants and Elastic Moduli of Metals and Insulators*, ed. I N Frantsevich (Kiev: Naukova Dumka) pp. 60–180
[25] Pugh S F 1954 *Philos. Mag*. **45** 823